IOP Publishing J. Phys. D: Appl. Phys. 59 (2026) 105502 https://doi.org/10.1088/1361-6463/ae4910

Journal of Physics D: Applied Physics

PAPER

AC field driven interactions in concentrated electrolytes

Carla S Perez-Martinez[1,*], Timothy S Groves[2], Marco Balabajew[3], Christian D van Engers[4], Nico Cousens[5], Florian Hausen[6,7], Alexander M Smith[5] and Susan Perkin[2]

[1] London Centre for Nanotechnology, University College London, 17-19 Gordon Street, London WC1H 0AH, United Kingdom
[2] Physical and Theoretical Chemistry Laboratory, University of Oxford, South Parks Road, Oxford OX1 3QZ, United Kingdom
[3] TNG Technology Consulting GmbH, Beta-Str. 13, 85774 Unterföhring, Germany
[4] Centre for Microscopy and Microanalysis, University of Queensland, St. Lucia 4072, Australia
[5] Independent Researcher, London, United Kingdom
[6] Institute of Energy Technologies IET-1, Forschungszentrum Jülich GmbH, 52425 Jülich, Germany
[7] Institute of Physical Chemistry, RWTH Aachen University, 52074 Aachen, Germany
[*] Author to whom any correspondence should be addressed.

E-mail: carla.perezmartinez@ucl.ac.uk

Keywords: ionic liquids, concentrated electrolytes, AC fields, surface force balance

Supplementary material for this article is available online

OPEN ACCESS

RECEIVED
1 December 2025

REVISED
10 February 2026

ACCEPTED FOR PUBLICATION
23 February 2026

PUBLISHED
9 March 2026

Abstract

Using a surface force balance, we measure the force between two crossed-cylinder electrodes for different electrolyte systems and different geometrical configurations under the influence of an AC field. When an AC field is applied to concentrated mixtures of an ionic liquid (IL) in a polar solvent, a force arises that is at least an order of magnitude larger and slower to reach steady state than the static response of the electrolyte. We demonstrate that this AC field effect persists in concentrated electrolytes beyond what has already been observed in pure ILs or aqueous electrolytes. Furthermore, we show that the magnitude of the electric field force response is dependent on the electrode radius of curvature. In experiments with pure ILs, a stronger force magnitude is observed for a smaller radius of curvature, implying that these interactions can be fine-tuned through geometrical design. These observations should guide the application of AC electric fields for the control of colloids and the design of passive control mechanisms in microfluidics and nanotribology.

1. Introduction

The control of electrolyte systems with electric fields has a plethora of technological applications, ranging from the assembly of colloids [1, 2], AC electroosmosis and pumping in microfluidics [3, 4], to the control of adhesion and friction [5, 6]. Electric fields are ubiquitous in energy storage and catalysis and are routinely used in the characterisation of these systems via electrochemical impedance spectroscopy [7]. Understanding the effect of fields on electrolytes is more relevant than ever as the emerging field of iontronics seeks to create ionic machines for computation, sensing, and filtration [8, 9].

The surface force balance (SFB) provides a platform for the study of the effects of electric fields on electrolytes in confinement. In its most standard configuration, a liquid is confined between two atomically smooth mica surfaces set in crossed-cylinder geometry. The backs of the mica surfaces are coated in a semi-transparent thin silver layer. Interferometry is used in the silver–mica–liquid–mica–silver stack for the detection of the interaction forces and distance between the two mica surfaces [10]. The surfaces can be moved towards and away from each other, allowing the measurement of surface forces as a function of distance, or sheared against one another, allowing the measurement of friction and shear forces. The silver mirrors can be used to apply electric fields by connecting them to a power supply. Drummond [11] was the first to use the silver mirrors simultaneously as electrodes, demonstrating electric field induced friction reduction and control on polymer brushes deposited on the mica surfaces [11].

Perez-Martinez and Perkin [12] used the SFB to study the effect of AC fields on thin films of ionic liquid (IL). When an IL is confined between mica surfaces, and the silver mirrors are used as electrodes to apply an AC field, the field induces a force that diverges substantially from the calculated static

response of the electrolyte [12]. This study found that the magnitude of the force is larger than predicted, that the force can be either attractive or repulsive, and that the system approached steady state on timescales of 100–1000 s, which is significantly slower than the charging and viscous timescales of the system [12]. Additionally, it was observed that when the field is turned off, the system relaxes back to its original state on a similarly slow timescale [12].

In that same work, in order to eliminate any variability arising from specific effects of the mica surfaces, Perez-Martinez and Perkin [12] replaced the back-silvered mica with gold surfaces. Characterisation experiments were performed with IL confined between two gold surfaces, with the gold surfaces acting simultaneously as electrodes and mirrors for interferometry. A similar phenomenon was observed in the gold–gold setup. It was determined that the magnitude and response time of the observed force are independent of the separation distance between the surfaces (in the tens of micrometres range) or the frequency of the applied electric field [12]. Furthermore, the magnitude of the force scales with the square of the applied voltage [12].

Richter *et al* [13] have reported a similar phenomenon in dilute aqueous electrolytes [13]. In their experiments, the solutions are confined between mica surfaces, and a long-range repulsive force is always observed when an AC field is applied. As with ILs, the timescale for the response to the AC field of the aqueous electrolytes is of the order of a few minutes. Similarly to the results in [12], [13], found that the magnitude of the effect was independent of the surface separation or the driving frequency, and dependent on the square of the applied voltage. In addition, it was found that the magnitude of the effect was dependent on the difference in the diffusion coefficients of the ions in the aqueous electrolyte, with a larger effect magnitude observed for more disparate diffusivities [13]. In order to explain the observed effect in aqueous electrolytes, Richter *et al* [13] derived a model making use of the Poisson–Nernst–Planck equations to determine ion concentrations in a 1D capacitor under an electric field. When an AC field is applied, they found that 'both cations and anions accumulate on average in the vicinity of the electrode', in contrast to the DC case where only counterions accumulate at the charged surface. The magnitude of the ion excess is proportional to the square of the applied voltage. The experimentally observed force response was explained as resulting from an increase in osmotic pressure, which is generated as the field drives an excess of cations and anions through lateral transport from adjacent reservoirs. The model predicts an increase in excess ion concentration and force magnitude with increasing bulk concentration. However, the model is not expected to hold at high bulk concentrations, and indeed the experimental data from [13] with aqueous $NaNO_3$ shows initially a stronger response as the concentration is increased up to 10 mM, but a decrease in response as the concentration is increased further.

The goal of this study is to elucidate if the phenomena observed in ILs and aqueous electrolytes subjected to AC electric fields extends to other systems, and the dependence of the effect on geometrical parameters. The paper presents measurements on concentrated mixtures of IL in a polar solvent and compares the effect to the pure IL response. The effect has also been studied for a pure IL in systems of varying geometry. To the best of our knowledge, the influence of geometry on the observed effect has not been studied, and this work finds that the effect is dependent on the system's radius of curvature. Section 2 describes the experimental setup. Section 3 presents the results, and section 4 reviews the observations in comparison to additional work from the literature that aims to explain the phenomena.

2. Experimental methods

We use a simplified SFB setup, using gold lenses, to study the dependence of the electric field effect on liquid composition and geometrical factors. In the SFB, a thin liquid film is confined in between two hemi-cylindrical lenses, as shown in figure 1(a).

The fused silica lenses are each coated with a 2 nm layer of chromium and a 40 nm layer of gold. These metals are deposited via thermal evaporation using an Edwards Auto 306 Cryo Evaporator. The gold layers function both as mirrors for interferometry and as electrodes for applying the AC electric field. When white light is shone through the setup, interferences in the cavity formed by the two lenses produce a pattern of fringes of equal chromatic order (FECO) when emerging light is directed onto a spectrometer grating. The FECO pattern is used to determine the distance between the surfaces, D, as well as the effective radius of curvature of the setup, R. More details on the FECO calculations are provided in the supplementary information. The lenses are cleaned in piranha solution, rinsed in ultrapure water, stored in ethanol, and dried with nitrogen prior to use.

The bottom lens is mounted in a small polytetrafluoroethylene (PTFE) cup, which in turn is mounted on a leaf spring of known stiffness k, as shown in figure 1(b). The deflection of the spring, δ, can be inferred from the FECO pattern, thus giving the interaction force between the surfaces, $F = k\delta$.

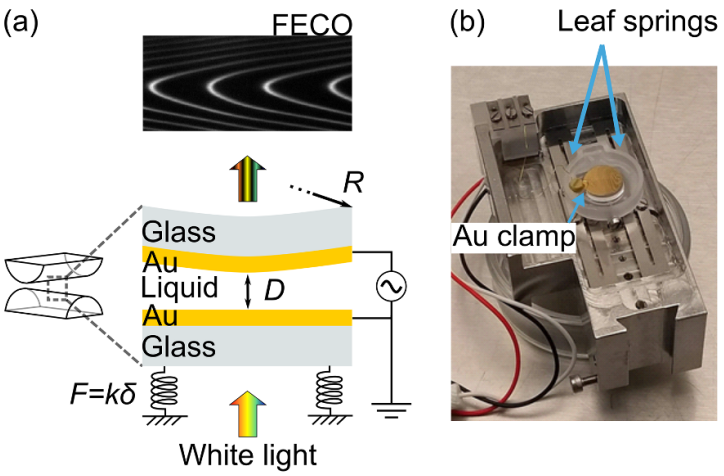

Figure 1. (a) SFB experimental geometry. Two hemi-cylindrical lenses are placed facing each other; the lenses have a thin coating of gold that acts as both an electrode and a mirror for interferometry. The cross-cylinder experimental geometry has an effective radius of curvature R. White light is shone through the setup, and the resulting pattern of fringes of equal chromatic order (FECO) can be analysed to determine the minimum separation between the electrodes, D. (b) Photograph of a lens mounted in the setup. The image corresponds to the bottom lens. The lens sits in a small PTFE cup, which in turn sits on a set of horizontal leaf springs. The gold surface is connected to an electric field generator via a thin gold wire held in place by a gold clamp.

Electric fields are applied normal to the liquid film. To make the electrical connections, a thin Au wire is contacted to each lens using a small clamp made of bouillon gold (99.9% purity). The gold wires (Goodfellow) are 0.125 mm conductor diameter (99.99% purity), with a PTFE coating of 0.016 mm thickness. A Keysight 33500B signal generator is used to apply the voltages to the electrodes; the bottom electrode is held at the ground of the chamber through the signal generator, while bias is applied to the top electrode. The fields are generated by applying a sinusoidal voltage of root-mean-square amplitude V_0 and frequency ν. A typical applied frequency was 10 kHz, but frequencies ranging from about 500 Hz to 1 MHz were also tested. The supplementary information explains why electrochemical reactions are not expected to affect the measurements reported here at $\nu \geqslant 5$ kHz, and documents conditions under which degradation was observed and therefore excluded from analysis.

The quality of the electrical connections was checked in air prior to injection of the liquid. The magnitude of the spring deflection in air when subjected to either DC or AC fields checks well with the prediction from the model developed in [12], without need for fitting parameters.

Experiments were then performed with the following test liquids:

(i) A pure IL, 1-butyl-1-methylpyrrolidinium bis(trifluoromethylsulfonyl)imide ([C_4C_1Pyrr][TFSI], Iolitec 99.5%)
(ii) A 2 mol l^{-1} (M) mixture of [C_4C_1Pyrr][TFSI] with Propylene Carbonate (PC, Sigma-Aldrich, anhydrous, 99.7%).
(iii) A 0.7 mol l^{-1} mixture of [C_4C_1Pyrr][TFSI] with PC

Prior to experiments, the IL is dried *in vacuo* ($<5 \times 10^{-3}$ mbar) at 80 °C for at least 12 h. Propylene carbonate is taken from freshly opened bottles for each experiment, and mixtures with IL are swiftly prepared to minimise water uptake prior to experiments. The supplementary information includes some additional notes on the mixture preparation, the molarity and molality calculations, and the refractive indices of the solutions used in the FECO analysis.

Approximately 100 μl of test liquid is injected in between the lenses, which is sufficient to ensure the liquid completely bridges the gap between the lenses and a small excess overflows onto the surrounding PTFE cup. After injection, a small amount of desiccant (phosphorous pentoxide, Sigma Aldrich, 99%) is introduced into the chamber and the chamber is sealed.

Experiments with a given set of lenses and injected liquid are conducted over a span of one to 3 d, during which the chamber remains sealed. Evaporation is not a concern with pure ILs, but may occur with the IL/PC mixtures. The supplementary information provides further details on the specific experiments reported and notes small variations observed for the measurements with the 0.7 M mixture over the span of the experiment, which may be due to some limited evaporation. At the end of an

experiment, the chamber is opened, the test liquid is rinsed away with ethanol, and the lenses and holders are cleaned with solvents and acid baths prior to use in another experiment.

A typical run measuring the response of the system on the application of the electric field involved placing the surfaces at a chosen starting separation, D_0, using a mechanical or piezoelectric drive. The distance was recorded for at least 30 s before applying a voltage at $t = 0$. The response of the system was recorded until steady state was reached. Once the surface separation was constant, the voltage was turned off, and the relaxation of the system was recorded. The recording period for each experimental run is one to two hours, and drift is likely to occur over this timescale due to thermal fluctuations of the instrument, despite the room being temperature controlled and held at 21 °C. Therefore, some of the $D(t)$ data have been corrected to subtract a linear drift where necessary.

3. Results

3.1. AC field effect on IL/PC systems

When an AC electric field is applied to mixtures of $[C_4C_1Pyrr][TFSI]$ in PC in the Au–Au SFB setup, a response similar to that reported in [12, 13] is observed. Figure 2(a) shows several experiments where an AC electric field is applied to the 2 M solution of $[C_4C_1Pyrr][TFSI]$ in PC. The figure shows the force F, normalised by the surface radius of curvature R, as a function of time, for four different runs where the applied voltage V_0 was varied whilst keeping the starting distance and driving frequency constant ($D_0 \approx 16\,\mu$m, $\nu = 10$ kHz). In figure 2(a), the electric field is turned on at $t = 0$ as indicated by the dotted line, and turned off as indicated by the short dotted lines along each experimental curve. When the field is turned on, the surfaces approach each other, $D(t)$ decreases, giving rise to a negative F (overall attractive force). As shown in this figure, the force reaches steady state in a timescale of several hundred seconds. We denote the force between the surfaces at steady state in the applied AC field as F_{ss}. When the field is turned off, the process is reversed, and the surfaces return to their original separation on a similar timescale. The process may not always be exactly symmetric as it can be difficult to completely remove thermal drift from experimental runs spanning about two hours. The data showing the micrometer level displacement of the surfaces, $D(t)$, for the experimental runs shown in figure 2(a), is shown in the supplementary information.

Additional onset phenomena—here referred to as transients, consisting of quick attractions/repulsions before the strong, slow effect—have been reported previously but are not as obvious for the particular experimental run reported in figure 2(a). These onset processes have been observed in other experiments with this same liquid (see supplementary information) and for the other liquids used in this study, however, the onset transients are small compared to the overall phenomenon and this work focuses on the largest effect observed.

We will proceed to argue that the magnitude of the effect, F_{ss}, is several times larger than what would be expected from the electrolyte were it to behave as a perfect dielectric fluid. In [12], the theoretical value of the steady-state force $F_{calc,ss}$ of a perfect dielectric liquid, of relative permittivity ϵ, subjected to a high-frequency AC field in the SFB, for separations $D \ll R$, was derived as

$$F_{calc,ss}/R = \frac{\epsilon \pi V_0^2}{2D_0}. \tag{1}$$

The dielectric constant of the mixture of IL in PC is not available in the literature; however, the extremes of the dielectric behaviour for the mixture can be taken from the pure liquids to use in estimating $F_{calc,ss}/R$ from equation (1). The relative dielectric permittivity of $[C_4C_1Pyrr][TFSI]$ is 14.7 (25° [14]) and for PC, the value is approximately 66 (25° [15]). In the strongest possible response, if the liquid dielectric constant was taken to be the maximum value for PC, the value of $F_{calc,ss}/R$ would be 0.7 and 5.5 mN m^{-1} for $V_0 = 2.5$ and 7 V_{RMS}, respectively. The observed values of F_{ss}/R, as shown in figure 2(a) are at least an order of magnitude larger than the upper bound theoretical estimation from the perfect dielectric scenario.

Similar experiments were performed with the 0.7 M mixture of $[C_4C_1Pyrr][TFSI]$ in PC, at two frequencies, 10 kHz and 1 MHz. A strong overall attractive response was observed for this more dilute system, as well as a dependence on the applied voltage at both applied frequencies. The runs for the 0.7 M mixture of $[C_4C_1Pyrr][TFSI]$ in PC are included in the supplementary information.

Two additional experiments of the neat $[C_4C_1Pyrr][TFSI]$ in the Au–Au SFB are reported in this work. The previously reported experiment for this liquid in [12] had shown an overall repulsive force upon application of the electric field, and the two new experiments reported here display an overall attractive force. An example voltage sweep for the neat IL is shown in the supplementary information,

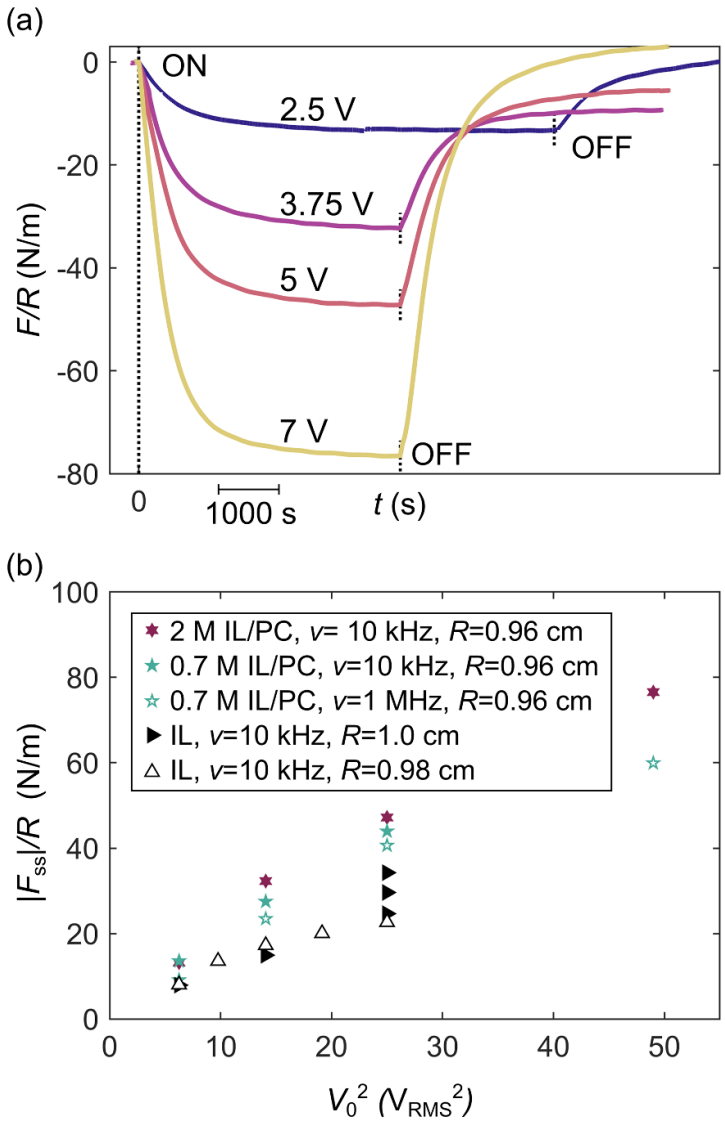

Figure 2. (a) Response of 2 M mixtures of [C_4C_1Pyrr][TFSI] in PC to an AC electric field. The traces show F/R as a function of time, measured for a range of different driving voltages V_0 (in RMS values) as indicated next to each curve. The electric field is turned on at $t = 0$ as indicated by the dotted line. Before the field is turned on, there is no net force. With the field on, an overall attractive force arises. The field is turned off at the point indicated by the shorter dotted line along each curve (after 7200 s for the 2.5 V run, and 4500 s for the other runs). (b) Steady-state force, F_{ss} normalised by the radius of curvature R, measured upon application of the electric field to the pure ionic liquid [C_4C_1Pyrr][TFSI] and to mixtures of this ionic liquid in propylene carbonate. For both panels in this figure, $D_0 = 16\,\mu$m, $R \approx 1$ cm, and $\nu = 10$ kHz unless noted otherwise.

alongside a comparison to the predicted theoretical model from [12], showing the steady-state force magnitude is at least an order of magnitude stronger than predicted by the model.

From the four runs shown in figure 2(a) for the 2 M mixture, it is evident that the magnitude of the electric field response, F_{ss}, depends on the applied voltage magnitude V_0. This dependence was also observed in the 0.7 M mixture and the neat IL. The dependence of F_{ss}/R as a function of V_0^2 for the three test liquids is plotted in figure 2(b). For simplicity and consistency, we limit our comparison to experiments showing an overall attraction. As can be observed, for a given voltage, the response of the 2 M solution is usually strongest, albeit not significantly different from the 0.7 M solution, and both of these are greater in magnitude to the response of the neat IL. For each test liquid, the magnitude of the response seems to scale with the square of the applied voltage, in agreement with previous measurements in pure ILs and dilute aqueous solutions [12, 13].

Besides studying the dependence of the response of the different liquids to changes in V_0, this work has also determined that the effect seems to be independent of D_0 or ν for the liquids studied. Experimental sweeps were performed with the pure IL and the 0.7 and 2 M IL/PC systems, where the effect was measured whilst varying D_0 or ν and keeping other parameters constant. The measured responses are included in the supplementary information, where it can be observed that the measured

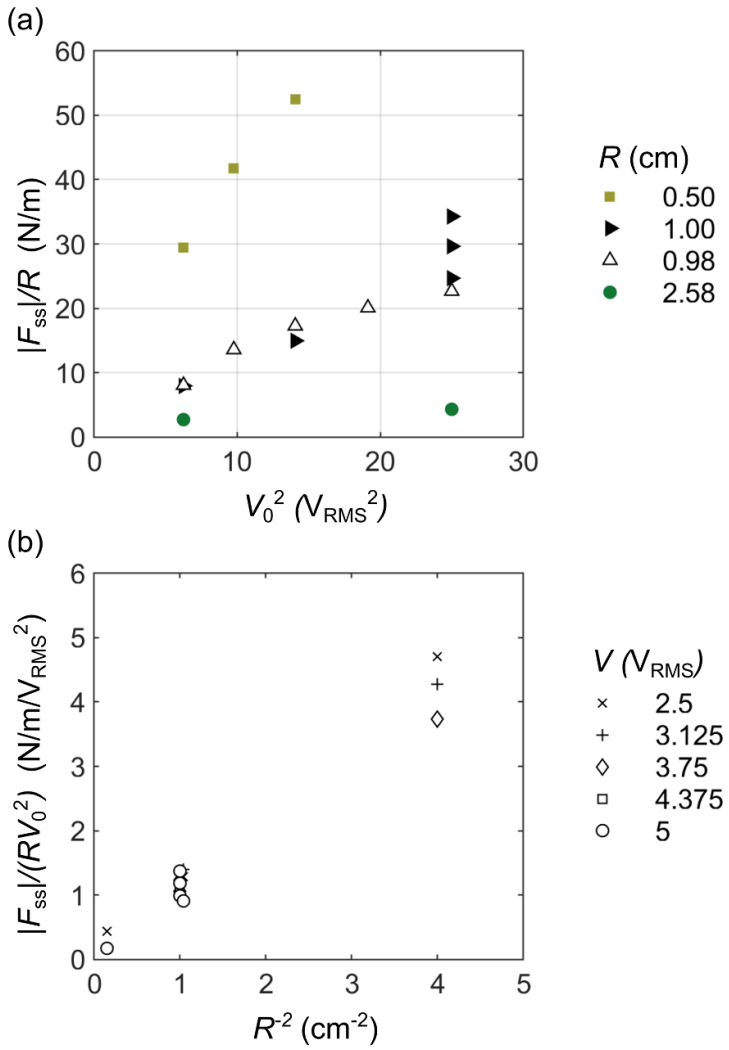

Figure 3. (a) Steady-state force, F_{ss} normalised by the radius of curvature R, measured upon application of the electric field to the pure ionic liquid [C_4C_1Pyrr][TFSI], as a function of applied voltage, in setups of different R. The data points were taken with $D_0 = 16\,\mu$m and $\nu = 10$ kHz. (b) Radius dependence of the measured effect. The steady-state force F_{ss} is normalised by RV_0^2 to decouple the effect of the applied voltage from the effect of R.

effect is independent of D_0 (typically varied in the range 8–70 μm $\ll R$) and ν (ranging mostly between 5 kHz and 1 MHz). The observation that the AC electric field response is independent of D_0 or ν is also consistent with previous work [12, 13].

3.2. AC field response dependence on *R*

Geometry dependence studies were performed with the IL [C_4C_1Pyrr][TFSI] confined between lenses with radius of curvature $R = 0.50, 0.98, 1.00$ and 2.58 cm. The overall shape of the electric field response for the $R = 0.50$ and 2.58 cm is very similar to that observed with the $R = 1$ or 0.98 cm setups (see supplementary information for full traces of $F(t)/R$). When the electric field is turned on, there is a transient of a few tens of seconds, consisting of an attraction and a repulsion, that then gives way to an overall, larger, attractive force which develops over a slower timescale (hundreds of s). When the electric field is turned off, the phenomenon is reversed. A quick, small repulsion is followed by a quick attraction, before the force becomes overall repulsive and restores the system back to its original state.

The magnitude of the overall response is compared at different set voltages V_0 (and fixed starting distance and frequency) while varying R. Figure 3(a) shows F_{ss}/R as a function of V_0^2 for the different experimental R considered. The magnitude of the response increases with V_0^2 for all R. Furthermore, it is evident that for a given voltage, F_{ss}/R is greater the smaller R. Interestingly, for a dielectric liquid in the SFB, the normalised force F/R should be independent of R (equation (1)). The calibration tests in air prior to IL injection do in fact obey the dielectric model. However, when an AC field is applied to the IL, the magnitude of the effect increases with decreasing R.

The dependence of the electric field response on R is even more striking when one normalises F_{ss}/R by V_0^2, and plots the measurements as a function of R^{-2}. As shown in figure 3(b), the data points group together for each value of R. There is some uncertainty in the value of F_{ss} measured in each experiment due to thermal drift over the long timescales required for reaching steady state; however, it is clear from the data that the geometry plays an important role in the measured effect. Note that the effective radius R, rather than the electrode surface area, is believed to be the main geometrical factor; in fact, the areas of the gold surface are 1, 0.79 and 0.81 cm^2, for $R = 0.5, 1$ and 2.58 cm respectively (calculated using Solidworks software) and do not vary greatly between experiments.

The dependence of the AC field response to other parameters (frequency and starting separation) was studied at $R = 2.58$ cm, and is shown in the supplementary information. These experiments indicate that the effect is not dependent on starting distance or driving frequency. The experiments with the smaller radius were limited to a voltage sweep, as increasing the voltage beyond 3.75 V_{RMS} led to degradation of the gold surfaces.

4. Discussion

The main conclusions from the experiments reported are as follows:

- An AC electric field applied to pure ILs or to mixtures of IL with polar solvent in the crossed-cylinder configuration of the SFB results in a force that is stronger in magnitude than the calculated static response of the electrolyte.
- For all liquids tested, the effect magnitude scales with the square of the voltage, but appears to be independent of the starting separation D_0 between the surfaces or of the driving frequency.
- The strength of the electric field response is highly dependent on the radius of curvature of the surfaces, with a stronger response for a smaller radius of curvature.
- The response of the system to the AC electric field takes place over a timescale of several 100 s.

The long relaxation times observed may suggest diffusive transport over meso or macroscopic lengthscales. The RC charging time of the double layer depends on the Debye length, cell geometry, and effective diffusivity [16–18], and is only of the order of 10^{-2} s [12]. This fast timescale is not resolved in our measurements, and the measured hundreds-of-seconds dynamics cannot be attributed to RC charging. Recent theoretical works hint at longer timescales in play. Balu and Khair [19] considered the charging of a cell with a concentrated electrolyte in between parallel electrodes separated by a distance L under a suddenly applied DC voltage (small in magnitude compared to the thermal voltage). The authors included Stefan–Maxwell fluxes in the derivation of modified Poisson–Nernst–Planck equations, and discovered that there are two charging timescales: the standard RC time, and a longer timescale, $L^2/\mathscr{D}_a$, where $\mathscr{D}_a$ is the ambipolar diffusivity of the salt. Ma *et al* [20] used dynamic density functional theory to study the charging of a planar electrode capacitor with concentrated electrolytes after a square-step voltage is applied to the electrodes. Their model assumes both the cations and anions have equal diffusivities and sizes, but does take into account ion–ion correlations, packing effects, and dispersion forces, which are relevant in concentrated electrolytes. As in the work of Balu and Khair, the electrode charge forms exponentially with two timescales, first, the RC charging time, and then the diffusion time $L^2/\mathscr{D}$, with $\mathscr{D}$ the diffusivity of the electrolyte under consideration.

What is the relevant lengthscale L for diffusion in the setup presented in this paper? For curved surfaces, one could expect that the radius of curvature of the system should play a role, and a timescale $\sim R\Lambda/\mathscr{D}$ could be plausible, with Λ a lengthscale that will be discussed shortly. There is a limited set of data for comparing the effect of R on the timescale needed for reaching steady state, namely, the runs with $V_0 = 2.5\,V_{RMS}$, $D_0 = 16\,\mu$m, $\nu = 10$ kHz, where R has been varied. The data for these runs have been fitted with exponential functions of the form $F(t) = F_{ss}(1 - \exp -t/\tau_{ss})$, as shown in the supplementary information, to obtain the time needed for the system to reach steady state, τ_{ss}. For $R = 0.50$, 1.00, 0.98 and 2.58 cm, $\tau_{ss} = 495$, 655, 678 and 899 s, respectively. Although these numbers seem to indicate some correlation of τ_{ss} with R, this observation should be interpreted with caution, as the exponential fits are not of optimal quality due to drift and there is limited data to support this conclusion. Whilst R could play a role in the system dynamics, there is still the question of the other relevant lengthscale Λ. The effect being independent of starting distance suggests that this Λ is not related to D_0, and that this quantity is more or less constant for the experiments considered here. Given the timescale for relaxation of $\sim$500 s, an IL diffusivity of 5×10^{-11} $m^2\,s^{-1}$ [21], and a typical R of 1 cm, Λ should be about 2.5 μm—a dimension of about a tenth of the gap sizes considered in the experiment.

Recent works provide some possible explanations to account for the mechanism of the response of electrolyte systems to AC fields. As explained in the introduction, the model from Richter *et al* shows a build-up of excess ion concentrations under the AC fields [13], and even though the assumptions of this model may break down at the concentrations reported in this work, the concentration build-up mechanism may be at play in the systems under consideration. Hashemi *et al* [22] have found that applying an oscillatory field in a cell with parallel planar electrodes across a liquid containing ions with unequal mobilities generates a long-range steady electric field, which they call asymmetric rectified electric field, and which scales with the square of the applied voltage. Mahdisoltani and Golestanian [23] studied the dynamics of an electrolyte confined between two neutral walls and subjected to an electric field running parallel to the walls. In this scenario, the field pushes the positive and negative ions in opposite directions, creating fluctuations in ion density that are long-ranged. These long-range correlations give rise to a fluctuation-induced force between the neutral walls. This fluctuation induced force can be either attractive or repulsive, depending on the strength of the applied electric field or the relative dielectric constants of the electrolyte and the confining wall material. Balu and Khair in 2020 [24] have also studied the dynamic double layer force for planar parallel electrodes separated by a dilute monovalent electrolyte. The system is subjected to a time oscillating voltage, but the magnitude of the applied voltage is small when compared to the thermal voltage. They find the force sign can depend on the driving frequency. For the step voltage, they find two charging scales, the RC and the diffusion timescale that accounts for unequal diffusivities.

The response we are studying involves concentrated, strongly correlated electrolytes, with ions of unequal diffusivities, in a scenario that is challenging to treat analytically or computationally: the application of an AC electric field with an applied voltage several times larger in magnitude than the thermal voltage k_BT (k_B is Boltzmann's constant, T the system temperature), on a curved, non-planar, geometry. Crucially, the strong dependence of the effect on the radius of curvature suggests that the effect is dependent on field gradients, so the geometry of the system plays a key role in the explanation of this phenomena. Future theoretical works should focus on the role of geometry in the observed AC effect. The work reported here should help inform the design of systems that take advantage of geometry for the control of colloids, microfluidics, and iontronics.

Acknowledgments

S P and C S P-M are grateful for funding from The Leverhulme Trust (RPG-2015-328) and the European Research Council (under starting Grant no. 676861, LIQUISWITCH). C S P-M further acknowledges support from a UKRI Future Leaders Fellowship (MR/S032312/1 and MR/Y034376/1). S P further acknowledges support from the European Research Council (under Grant 101001346 ELECTROLYTE). C v E is grateful for a Zvi and Ofra Meitar Magdalen Graduate Scholarship. F H is grateful for DFG Forschungsstipendium under HA7072/1-1. Thanks to James Hallet for sharing codes for processing some of the experimental data.

Data availability statement

All data that support the findings of this study are included within the article (and any supplementary files).

Supplementary Information available at https://doi.org/10.1088/1361-6463/ae4910/data1.

ORCID iDs

Carla S Perez-Martinez 0000-0002-5574-0319
Timothy S Groves 0000-0003-2168-2437
Marco Balabajew 0009-0001-2798-2521
Christian D van Engers 0009-0006-2033-0367
Alexander M Smith 0000-0001-5086-8164
Susan Perkin 0000-0002-5875-5217

References

[1] Edwards T D and Bevan M A 2014 *Langmuir* **30** 10793–803
[2] Bukosky S C, Hashemi A, Rader S P, Mora J, Miller G H and Ristenpart W D 2019 *Langmuir* **35** 6971–80
[3] Ramos A, Morgan H, Green N G and Castellanos A 1999 *J. Coll. Interf. Sci.* **217** 420–2
[4] Ajdari A 2000 *Phys. Rev. E* **61** R45–R48

[5] Perez-Martinez C S, Groves T S and Perkin S 2021 *J. Phys.: Condens. Matter* **33** 31LT02
[6] Bresme F, Kornyshev A A, Perkin S and Urbakh M 2022 *Nat. Mater.* **21** 848–58
[7] Lazanas A C and Prodromidis M I 2023 *ACS Meas. Sci. Au* **3** 162–93
[8] Bocquet L 2023 *Faraday Discuss.* **246** 618–22
[9] Liu Y, Peng P, Qian H, Wang Z L and Wei D 2025 *Nano Res. Energy* **4** e9120156
[10] Hayler H J, Groves T S, Guerrini A, Southam A, Zheng W and Perkin S 2024 *Rep. Prog. Phys.* **87** 046601
[11] Drummond C 2012 *Phys. Rev. Lett.* **109** 154302
[12] Perez-Martinez C S and Perkin S 2019 *Soft Matter* **15** 4255–65
[13] Richter Ł, Żuk P J, Szymczak P, Paczesny J, Bąk K M, Szymborski T, Garstecki P, Stone H A, Hołyst R and Drummond C 2020 *Phys. Rev. Lett.* **125** 056001
[14] Huang M M, Jiang Y, Sasisanker P, Driver G W and Weingärtner H 2011 *J. Chem. Eng. Data* **56** 1494–9
[15] Chernyak Y 2006 *J. Chem. Eng. Data* **51** 416–8
[16] Bazant M Z, Thornton K and Ajdari A 2004 *Phys. Rev. E* **70** 021506
[17] Tivony R, Safran S, Pincus P, Silbert G and Klein J 2018 *Nat. Commun.* **9** 1–8
[18] Janssen M 2019 *Phys. Rev. E* **100** 042602
[19] Balu B and Khair A S 2018 *Soft Matter* **14** 8267–75
[20] Ma K, Janssen M, Lian C and van Roij R 2022 *J. Chem. Phys.* **156** 084101
[21] Tokuda H, Tsuzuki S, Susan M A B H, Hayamizu K and Watanabe M 2006 *J. Phys. Chem. B* **110** 2833–9
[22] Hashemi A, Bukosky S C, Rader S P, Ristenpart W D and Miller G H 2018 *Phys. Rev. Lett.* **121** 185504
[23] Mahdisoltani S and Golestanian R 2021 *Phys. Rev. Lett.* **126** 158002
[24] Balu B and Khair A S 2020 *Phys. Rev. Res.* **2** 013138